

Self-generated gradients stabilize the hydrodynamic instabilities in active suspensions

Mehrana R. Nejad¹ and Ali Najafi^{1,2,*}

¹*Department of Physics, Institute for Advanced Studies in Basic Sciences (IASBS), Zanjan 45137-66731, Iran*

²*Research Center for Basic Sciences & Modern Technologies (RBST),*

Institute for Advanced Studies in Basic Sciences, Zanjan, Iran

(Dated: July 27, 2018)

Ordered phases emerged in active suspensions of polar swimmers are under long-wavelength hydrodynamic mediated instabilities. In this letter, we show that chemical molecules dissolved in aqueous suspensions, as an unavoidable part of most wet active systems, can mediate long-range interactions and subsequently stabilize the ordered phases. Chemoattractant in living suspensions and dissolved molecules producing phoretic forces in synthesized Janus suspensions are reminiscent of such molecules. Communication between swimmers through the gradients of such chemicals generated by individual swimmers, is the foundation of this stabilization mechanism. To classify the stable states of such active systems, we investigate the detailed phase diagrams for two classes of systems with momentum conserving and non-conserving dynamics. Our linear stability analysis shows how the stabilization mechanism can work for swimmers with different dynamical properties, e.g., pushers or pullers and with various static characteristics, e.g., spherical, oblate or prolate geometries.

Understanding and explaining the physics of active matter have attracted many interests recently [1–4]. Active suspensions, both living and synthetic systems, are not bounded by equilibrium laws, thus, show a variety of behaviors ranging from collective self organized motion (even in two dimension) [5–7] to nontrivial rheological properties [8–12]. Long-range rotational order, observed in active suspensions, are under strong dynamical instabilities mediated by hydrodynamic interactions in low Reynolds wet systems [5, 13]. This instability is generic in the sense that, it is not affected by any short-range interaction but its underlying mechanism is very sensitive to the hydrodynamic details of individual swimmers. For pushers (pullers), bend (splay) fluctuations diverge and initiate the instability. Interestingly and in contrast to this hydrodynamic mediated instability, there are examples that the ordered phases can be observed experimentally. Furthermore, studying stabilization mechanisms provides guidelines for designing micro swimmers exhibiting collective ordered motion. System-size dependent fluctuations in elastic systems [14] and 2-D film confinement [15, 16] provide mechanisms that can stabilize the instability.

In this article, we show that chemical signaling between swimmers is another potential mechanism that can stabilize the instabilities. Phenomena of taxis (chemo, photo and *etc.*) that are vital activities in most living organisms [17] and phoretic interactions between active agents in suspension of artificial swimmers [18, 19] can be considered as examples of such chemical signaling. Depending on the details of system under investigation, chemotaxis itself can initiate Keller-Segel type instabilities [20, 21] but there are examples showing that phoretic interactions between active agents can lead to interesting col-

lective behaviors [18, 22, 23]. Interplay between hydrodynamic and chemotaxis is investigated previously with a view on the effects of self generated flows on the stability of isotropic phase of auto-chemotactic swimmers [24]. In a different regime and at the threshold of hydrodynamic instabilities, we study the influence of chemotaxis on long wave-length instabilities. In both living and synthetic active matter, individual agents change their state of motion in response to a gradient in chemicals. Here we use a macroscopic phenomenological description in which, chemotaxis can be considered as currents proportional to the local gradient of concentration. Although, there are microscopic derivations that can support this picture [21, 25], chemotactic coefficients defined in this way can also be considered as parameters that can be measured experimentally. Extending the idea of phoretic Brownian particle [26] to both momentum conserving and non-conserving systems, we formulate a continuum description for an active suspension and use linear stability analysis to determine the stability criteria.

Let us consider an interacting suspension of swimmers moving in the presence of a concentration of chemical nutrients. Each swimmer is an axisymmetric particle with major and minor diameters given by ℓ and $\Delta\ell$ and it moves with an intrinsic speed given by v_0 along its major axis denoted by a unit vector \mathbf{m} . In a mean field description, the dynamics of this suspension is described by single particle probability distribution function $\psi(\mathbf{r}, \mathbf{m}, t)$, showing the probability to find a swimmer with orientation \mathbf{m} in position \mathbf{r} at time t . In addition to this distribution function, chemical concentration $c(\mathbf{r}, t)$ and velocity profile of the ambient fluid $\mathbf{u}(\mathbf{r}, t)$, created by moving swimmers, are dynamical variables that need to be determined. The Smoluchowski equation for ψ governs the dynamics of this interacting suspension:

$$\frac{\partial}{\partial t} \psi(\mathbf{r}, \mathbf{m}, t) + \nabla \cdot \mathbf{J}^t + \nabla_m \cdot \mathbf{J}^m + (\mathbf{m} \times \partial \mathbf{m}) \cdot \mathbf{J}_\perp^m = 0, \quad (1)$$

* najafi@iasbs.ac.ir

where ∇ and ∇_m stand for positional and orientational gradients. Denoting by \mathbf{D} and \mathbf{D}_r , the translational diffusion tensor and rotational diffusion coefficient of the swimmers, the currents are given by:

$$\mathbf{J}^t = [v\mathbf{m} + \mathbf{u} - D\nabla - (k_B T)^{-1} D\nabla U - \chi_t \nabla c]\psi,$$

$$\mathbf{J}_\perp^m = -[D_r(\mathbf{m} \times \partial \mathbf{m})(1 + \frac{U}{k_B T}) + \chi_r \mathbf{m} \times \nabla c]\psi,$$

and $\mathbf{J}^m = (\mathbf{I} - \mathbf{m}\mathbf{m}) \cdot (\boldsymbol{\Omega} + A\mathbf{G}) \cdot \mathbf{m}\psi$. Chemotaxis translational and rotational currents are introduced through phenomenological coefficients χ_t and χ_r , both can have positive or negative values. Symmetric and antisymmetric parts of the fluid velocity gradient are denoted by $2\mathbf{G} = \nabla \mathbf{u} + (\nabla \mathbf{u})^T$ and $2\boldsymbol{\Omega} = \nabla \mathbf{u} - (\nabla \mathbf{u})^T$ respectively. For axisymmetric swimmers we have $A = (1 - \Delta^2)/(1 + \Delta^2)$ [27]. In terms of distribution function, we define density $\rho = \int d\hat{\mathbf{m}}\psi$, polarization $\mathbf{P} = \int d\hat{\mathbf{m}}\psi \hat{\mathbf{m}}$ and nematic order parameter as: $\mathbf{Q} = \int d\hat{\mathbf{m}}\psi (\hat{\mathbf{m}}\hat{\mathbf{m}} - I/3)$. To take into account the hydrodynamic interactions, we consider the dynamics of fluid. Denoting the viscosity of ambient fluid by η , fluid flow obeys Stokes equation $\eta \nabla^2 \mathbf{u} - \nabla \Pi = \nabla \cdot \sigma^a$, that is supplemented by incompressibility condition $\nabla \cdot \mathbf{u} = 0$. Assuming that the swimmers are force-dipoles with strength ζ , their contribution to the Stokes equations appears as an active stress $\sigma^a = \zeta \mathbf{Q}$ [2]. For a dipolar swimmer, we assign $\zeta = 6\pi\eta\ell^2 v_0 \Delta_p$ where, Δ_p is a dimensionless number showing the strength of force-dipole associated with swimmer, for pusher $\Delta_p > 0$ and for puller $\Delta_p < 0$. Alternatively, to account for the hydrodynamic effects, an effective two-body interaction between swimmers can also be considered [28–30]. We also consider a short-range interaction potential as: $U = -\frac{4}{3}\pi\ell^3 U_0 (1 + \frac{\ell^2}{10} \nabla^2) \mathbf{m} \cdot \mathbf{P}$ with $U_0 > 0$ to introduce polar order in the suspension [31].

Considering both diffusion and convection, concentration of chemical molecules obeys the following equation: $\partial_t c(\mathbf{r}, t) = -\mathbf{u} \cdot \nabla c + D_c \nabla^2 c - K(c)\rho(\mathbf{r}, t) + S$ where, chemical molecules are injected to the medium through a uniform source term S and swimmers act as sinks for chemical molecules. Reaction rate K , is assumed to obey Michaelis-Menten kinetics, characteristic of catalytic reactions, as: $K(c) = K_0 c / (c + c_M)$ where K_0 is the maximum reaction rate and c_M denotes a concentration at which, the reaction rate reaches to its half maximum value [32–34]. The kinetics we are considering here is the simplest choice and there are other possibilities that we can consider as well without any crucial change in our final results.

To study the dynamics of fluctuations, we consider the case that our system fluctuates around a uniform distribution of both chemical nutrients and swimmers and set $c = c_0 + \delta c$ and $\rho = \rho_0 + \delta \rho$. For $t > 1/D_c$, system reaches to steady state and denoting the fluctuation wave vector by \mathbf{q} , the chemical concentration and velocity profile can be obtained explicitly as:

$$\tilde{\mathbf{u}} = \frac{i\zeta}{\eta q} (\hat{\mathbf{q}}\hat{\mathbf{q}} - \mathbf{I}) \cdot \delta \tilde{\mathbf{Q}} \cdot \hat{\mathbf{q}}, \quad \delta \tilde{c} = \frac{-K(c_0)}{D_c q^2 + \rho_0 \partial_c K} \delta \tilde{\rho}, \quad (2)$$

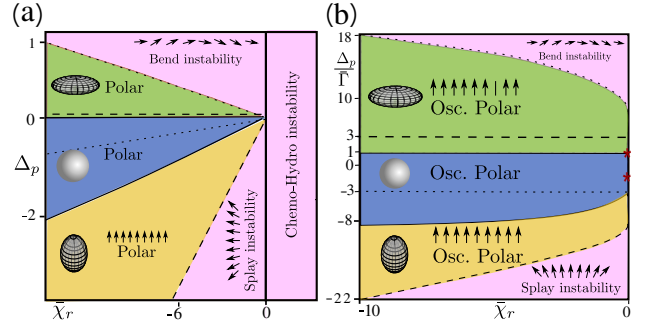


FIG. 1. (a) Stable regions for a 3-D momentum conserving polar suspension. In terms of Δ_p and $\bar{\chi}_r$, stable regions are shown for rod-shape, spherical and disk-shape swimmers. Boundaries of the stable regions are shown by dotted, solid and dashed lines for rod-shape, spherical and disk-shape swimmers respectively. (b) Regions of stability for a momentum non-conserving suspension interacting with substrate through friction coefficients $\bar{\Gamma}$ and $\bar{\Gamma}' < 0$. On the vertical axes, two highlighted points specify an interval $-\bar{\Gamma}_{min} < \Delta_p < \bar{\Gamma}_{max}$ where, the hydrodynamic screening stabilizes the system for $\bar{\Gamma}' < 0$ and $\bar{\chi}_t = \bar{\chi}_r = 0$. With short-range chemotaxis-assisted interaction, stable states will grow both for positive and negative values of $\bar{\Gamma}'$. Here, we have set $E = -2$ and $Pe = 1$.

where variables with tilde sign, show Fourier modes. In terms of chemical concentration, two different regimes of diffusion and reaction dominated can be distinguished. For sufficiently small concentrations $c_0 \ll c_M$, the dynamics of chemical molecules is totally governed by reaction process as: $\delta \tilde{c} = -(c_0/\rho_0)\delta \tilde{\rho}$ but for larger concentrations ($c_0 \geq c_M$), it is dominated by diffusion: $\delta \tilde{c} = -(K_0/D_c q^2)\delta \tilde{\rho}$. Having in hand the above results for $\delta \tilde{c}$ and $\tilde{\mathbf{u}}$, we can eliminate them from the Smoluchowski equation and obtain an equation that governs the dynamics of ψ . Instead of ψ , we can study the dynamics of its moments ρ , \mathbf{P} , \mathbf{Q} and higher moments. Cutting the hierarchical equations obtained with this method at the second order moment, will result in closed equations that show the dynamics of the system (details are given at the supplementary note).

As a result of short-range interactions, a transition from a homogeneous isotropic state with $\rho = \rho_0$ to a polar state with $\mathbf{P} = \rho_0 P_0 \hat{\mathbf{n}}$ will take place. To analyze the stability of polar state, we add small fluctuations $\delta \mathbf{n}$ and $\delta \rho$ to the steady state values then, study their linearized dynamics. Introducing the Fourier transform for any fluctuating field as $f(\mathbf{r}, t) = \int d\mathbf{q} d\omega \tilde{f}(\mathbf{q}) e^{i(\mathbf{q}\cdot\mathbf{r} - \omega t)}$ and denoting by θ the angle between $\hat{\mathbf{q}}$ and $\hat{\mathbf{n}}$, dimensionless modes can be obtained as: $\tilde{\omega} = a_1 \ell q \cos \theta + i h_\pm$ where,

$$h_\pm = g(\theta) \left[1 \pm \left(\frac{\sin^2 \theta (\bar{\chi}_r + i a_2 \ell q \cos \theta)}{g(\theta)^2} + (1 - \frac{2\bar{\chi}_t}{g(\theta)})^2 \right)^{\frac{1}{2}} \right]. \quad (3)$$

Characteristic frequency $\omega_0 = \frac{1}{2}\gamma \times (v_0/\ell)$ is used to make frequencies non-dimensional. Dimensionless phoretic co-

efficients are defined by:

$$\bar{\chi}_t = \frac{\chi_t}{2v_0\chi_0}, \quad \bar{\chi}_r = \frac{\chi_r}{\omega_0\chi_0}, \quad \chi_0 = \frac{D_c\omega_0}{\rho_0 K_0 v_0}, \quad \gamma = 3\pi\rho_0\ell^3,$$

$$g(\theta) = \Delta_p \cos 2\theta + \bar{\chi}_t, \quad a_2/\Delta_p = 2a_1 = 4\gamma^{-1}.$$

For simplicity we first begin by considering the spherical swimmers $A = 0$. Geometric effects for rod- or disk-like swimmers will be discussed at the end. The condition $\Im(\bar{\omega}) < 0$ ($\Re(\bar{\omega}) \neq 0$ or $= 0$) shows the stability criterion (oscillating or non-oscillating) and the onset of instability is given by the condition $\Im(\bar{\omega}) > 0$.

Well established results corresponding to the hydrodynamic mediated instability of polar phase can be seen by ignoring the chemotaxis in the above results [2, 5, 35]. Setting $q = \bar{\chi}_t = \bar{\chi}_r = 0$, we see that $\Im(\bar{\omega}) = 2\Delta_p \cos 2\theta$, showing that instability of pushers ($\Delta_p > 0$) and pullers ($\Delta_p < 0$) are due to bend ($\theta = 0$) and splay ($\theta = \pi/2$) fluctuations, respectively. Chemotaxis mediated instabilities in the absence of hydrodynamic interactions can also be investigated by setting $\Delta_p = q = 0$ that will result in $\Im(\bar{\omega}) = \bar{\chi}_t [1 \pm \Re(1 + \frac{\sin^2 \theta \bar{\chi}_r}{\bar{\chi}_t^2})^{\frac{1}{2}}]$. Regarding the signs of $\bar{\chi}_r$ and $\bar{\chi}_t$, we can distinguish different cases. When both of them are positive or one positive the other negative, it is easily seen that the homogeneous polar state is unstable. For $\bar{\chi}_t > 0$, chemotaxis collapse occurs that eventually makes the system inhomogeneous. For $\bar{\chi}_r > 0$, an instability in director (resulted from phoretic torque between swimmers) destroys polar order. Only the case where both chemotactic coefficients are negative ($\bar{\chi}_r < 0$, $\bar{\chi}_t < 0$), stable polar state is expected to observe in the system. In this regime, and for angles satisfying $\bar{\chi}_r \sin^2 \theta < -\bar{\chi}_t^2$, oscillating states can also be observed. Wave-number dependent oscillations of polar state in active matter have been studied before [36, 37]. Here, in addition to sound-like waves (terms proportional to a_1), wave-number independent ($q = 0$) oscillations of polar state is observed.

When both chemotaxis and hydrodynamics are considered, interesting results will appear. Regarding the above discussion and in terms of chemotactic coefficients, we expect to see non-trivial results when $\bar{\chi}_r < 0$, $\bar{\chi}_t < 0$. For a fixed and negative value of $\bar{\chi}_t$, fig. 1(a) shows a phase diagram of possible phases that can appear in a non-confined interacting suspension at the limit of $q = 0$. Chemotactic coefficient $\bar{\chi}_r$ and strength of hydrodynamic interactions Δ_p , are used to label the phase diagram. As seen from the phase diagram, chemotaxis can not completely suppress hydrodynamic instabilities of pushers ($\Delta_p > 0$) and a polar suspension of pushers is always unstable. Interestingly, chemotaxis can suppress the splay fluctuations and stabilize the polar state for pullers ($\Delta_p < 0$) and both static and oscillating polar phases can be seen at the phase diagram. Oscillations of polarized state observed in this phase diagram are scale-free in a sense that their frequency do not depend on wave-vector.

To have an intuitive picture about the stabilization mechanism, figures 2(a) and (b) show a collection of

nearly parallel swimmers that are under small bend and splay fluctuations, respectively. As seen from figures and as a result of such director distortions, density fluctuations will appear in the system. In terms of director fluctuations δn , density fluctuation for the case of splay is a first order effect but it is second order for bend distortion. In both cases, considering density fluctuations shows that, reoriented swimmers are much affected by the swimmers from left side where, their overall chemotactic torque tends to diminish fluctuations. Fluctuations suppression is much stronger for the splay case. To obtain this result, we have used the relation $-\bar{\chi}_r \mathbf{m} \times \nabla c$ with $\bar{\chi}_r < 0$ for chemotactic angular velocity and have assumed that at steady state, each swimmer consumes chemical molecules ($K_0 > 0$) and produce a radial gradient in chemicals. To prevent chemotactic collapse, it is necessary to consider $\bar{\chi}_t < 0$. For the case of bend fluctuations and at the first order of δn , chemotactic torques acting on distorted swimmers from left and right sides will cancel each other. Considering the higher order corrections, chemotaxis tends to diminish the fluctuations but, it is not so strong to remove the instability mediated from bend fluctuations in a system of pushers.

To investigate the stability of polar state in a system with finite size, we have plotted in fig. 2(c) and (d), the growth rate $\Im(\omega)$ as a function of θ for different values of q . Regarding the instability criterion $\Im(\omega) > 0$, fig. 2(c) shows that for pushers and at the absence of chemotaxis, the instability comes from bend modes ($\theta = 0, \pi$). Here, chemotaxis can suppress the fluctuations and make the instability angles more narrower but it is not able to totally remove the instability. This conclusion is valid for both infinite and finite systems. Fig. 2(d) shows that for pullers, and at $\bar{\chi}_r = \bar{\chi}_t = 0$, splay modes ($\theta = \pi/2$) diverges and initiate hydrodynamic instability. In this case chemotaxis can suppress the splay fluctuations for both infinite and finite system of pullers and eventually stabilize the system. Note that parameters are chosen from the stable region of phase diagram.

Elasticity that is identified by dimensionless bend and splay moduli \bar{K}_b and \bar{K}_s , is another interesting effect that can suppress the fluctuations. Including elasticity in our model, function $g(\theta)$ should be replaced by $g(\theta) = \Delta_p \cos 2\theta + \bar{\chi}_t - (q\ell)^2 (\bar{K}_s \sin^2 \theta + \bar{K}_b \cos^2 \theta)$ in equation 3. As shown in reference [14], elasticity introduces a length $L_b = \ell \sqrt{\bar{K}_b/\Delta_p}$, that systems with smaller sizes $L < L_b$, are stable against hydrodynamic fluctuations. Presence of chemotaxis does not change this picture for a suspension of pushers, but it enhances the threshold length scale. This elasticity induced stability mechanism for finite systems, works for the unstable part of the phase diagram presented in fig. 1(a).

To investigate the stability of isotropic state, we study the dynamics of fluctuations around a steady state given by $P = Q = 0$. For diffusion-dominated regime, linearizing the dynamical equations leads to the following modes

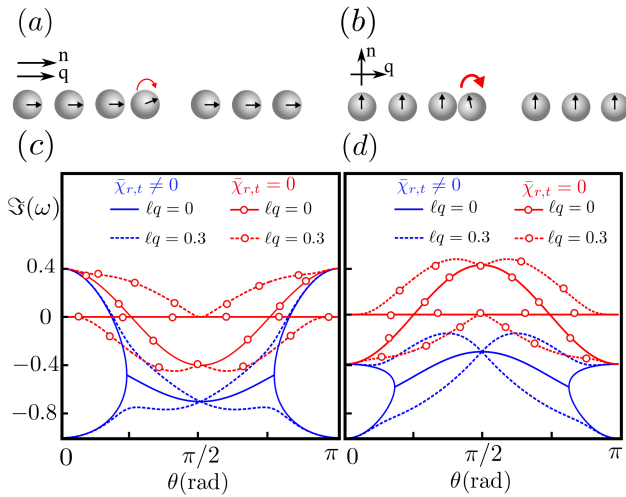


FIG. 2. (a) and (b) demonstrate how chemotaxis tends to suppress both bend and splay distortions in a suspension of spherical swimmers. As we can see, restoring torque (shown by curved red arrow) is more stronger for the case of splay fluctuations. (c) and (d) show the growth rate, $\Im(\omega)$, as a function of wave angle θ in a suspension of nearly aligned pushers and pullers, respectively. In the absence of chemotaxis (circled-red), bend distortions ($\theta = 0, \pi$) make pushers suspension unstable but for pullers it is splay fluctuation ($\theta = \pi/2$) that initiate the instability. Effects due to chemotaxis, shown as blue lines, strongly (weakly) diminish splay (bend) fluctuations for infinite and finite systems. Numerical values are $a_2 = 8$, $|\Delta_p| = 0.2$, $\bar{\chi}_r = -0.6$ and $\bar{\chi}_t = -0.5$.

for the fluctuations at $q = 0$:

$$\bar{\omega} = \left\{ i\bar{\chi}_t - i\bar{D} \pm i \left(\frac{2}{3}\bar{\chi}_r + (\bar{\chi}_t + \bar{D})^2 \right)^{\frac{1}{2}}, \frac{4i}{5}A\Delta_p - 6i\bar{D}_0 \right\},$$

where $\bar{D}_0 = D_r/\omega_0$, $\bar{D} = \bar{D}_0(1 - \rho_0/\rho^*)$ and $\rho^* = 9/(4\pi U_0 \ell^3)$. Stability of an isotropic suspension of swimmers depends not only on their type (pusher or puller), but also on their shape through parameter A . In the absence of chemotaxis and for $A\Delta_p > 15\bar{D}_0/2$, the isotropic state is unstable both for a suspension of pushers ($\Delta_p > 0$) with $A > 0$ and for pullers ($\Delta_p < 0$) with $A < 0$ [35, 37]. Isotropic suspension of spherical swimmers ($A = 0$) is always stable. As one can see from the above equation, modes associated to hydrodynamic and chemotaxis are independent and chemotaxis is not able to remove the instabilities. Taking into account the stability criterion for both hydrodynamic and chemotaxis part, we see that for $A\Delta_p < 15\bar{D}_0/2$, stable isotropic state can be observed under the condition $\bar{\chi}_t < \bar{D}$ and $\bar{\chi}_r < -6\bar{D}\bar{\chi}_t$.

Extending all the above results for reaction-dominated regime, shows that chemotaxis does not have any strong effect on the phase portrait of both polar and isotropic momentum conserving suspensions. In this regime, any local decrease in chemical molecules does not have enough time to diffuse and propagate to the position of other swimmers and subsequently chemotaxis is not able to re-

move hydrodynamic instabilities.

Friction with a substrate is another interesting and important factor in many experiments. Such friction can remove the instabilities by screening the long-range hydrodynamic interactions [38]. To study the dynamics of a suspension that is in contact with substrate, we replace the Stokes equation by: $-\Gamma\mathbf{u} - \nabla\Pi = \zeta_{2D}\nabla \cdot \mathbf{Q} + \Gamma'\mathbf{P}$ where $\Gamma(> 0)$ and Γ' are two phenomenological friction coefficients for the fluid and swimmers respectively [39, 40]. For diffusion-dominated regime, neglecting the effects of convection, as a result of hydrodynamic screening, polar suspension is always stable. For reaction-dominated regime both hydrodynamic and chemotaxis appear as short-range effects. Stable states of the suspension for this case, is presented in phase-diagram fig. 1(b) where, we investigate the stability criterion for different values of friction and rotational chemotaxis coefficients. Friction coefficient enters through a dimensionless variable given by $\Delta_p/\bar{\Gamma}$ with $\bar{\Gamma} = \Gamma\ell^2/\eta$. At the absence of chemotaxis ($\bar{\chi}_r = \bar{\chi}_t = 0$) and for $\Gamma' < 0$, friction can stabilize the suspension. This stability occurs in an interval given by $-\bar{\Gamma}_{min} < \Delta_p < \bar{\Gamma}_{max}$, denoted by two highlighted points on the vertical axis. By turning on the chemotaxis, both rotational and translational, available stable states will grow for $\Gamma' < 0$. For $\Gamma' > 0$ and at the presence of chemotaxis, there is also a stable region that is shown in fig. 1(b).

To analyze the stability criteria for non-symmetric swimmers, we set $A \neq 0$ and study the fluctuations spectrum. Detail analysis show that, in comparison to the spherical swimmers, hydrodynamic fluctuations are weaker in both rod-shape pullers and disk-shape pushers. This result holds for both momentum conserving and momentum non-conserving systems. As a result, depending on the geometry of swimmers, chemotaxis can stabilize both pusher and puller suspensions. Results for both prolate and oblate swimmers are reflected in fig. 1.

To estimate the range of chemotactic coefficients in micron scale systems, we note that the chemotactic velocity has the same order of magnitude as the swimming speed thus, $\chi_t \sim v_0\ell/c$. For a swimmer with $v_0 = 50\mu\text{m/s}$ and $\ell = 5\mu\text{m}$, moving in a $10\mu\text{M}$ concentration of food molecules with $D_c \sim 5 \times 10^{-10}\text{m}^2/\text{s}$, we can estimate the dimensionless chemotactic coefficients defined in equation (3) as: $\bar{\chi}_t \sim \bar{\chi}_r \sim \mathcal{O}(1)$. Here we have used $K_0 \sim 10^3\text{s}^{-1}$ and $\rho_0 \sim 10^{16}\text{m}^{-3}$. This estimation shows that our choice of parameters in fig. 1, can cover most real systems.

In conclusion, we have studied the role of chemotactic interaction in both wet and dry active systems and have shown that for both pushers and pullers, chemotaxis can suppress fluctuations. In a bulk of fluid, this suppression is much stronger for pullers and can develop a stable region in their phase diagram for various geometries of swimmers. For pushers in bulk fluid, chemotaxis can stabilize suspension of disk-shape swimmers. In the presence of a substrate and for small chemical Péclet number, long-range chemotactic interaction

can stabilize both puller and pusher suspensions when $\bar{\chi}_t, \bar{\chi}_r < 0$. In the case of finite Péclet number (presented in fig. 1(b), chemotaxis-assisted interaction can stabilize

hydrodynamic fluctuations.

Helpful discussions with S. Ramaswamy are gratefully acknowledged.

-
- [1] T. Vicsek and A. Zafeiris, *Physics Reports* **517**, 71 (2012).
- [2] M. C. Marchetti, J.-F. Joanny, S. Ramaswamy, T. B. Liverpool, J. Prost, M. Rao, and R. A. Simha, *Reviews of Modern Physics* **85**, 1143 (2013).
- [3] S. Ramaswamy, *Annual Review of Condensed Matter Physics* **1**, 323 (2010).
- [4] F. Jülicher, K. Kruse, J. Prost, and J.-F. Joanny, *Physics Reports* **449**, 3 (2007).
- [5] R. A. Simha and S. Ramaswamy, *Phys. Rev. Lett.* **89**, 058101 (2002).
- [6] T. Bickel, G. Zecua, and A. Würger, *Phys. Rev. E* **89**, 050303 (2014).
- [7] T. Vicsek, A. Czirok, E. Ben-Jacob, I. Cohen, and O. Shochet, *Phys. Rev. Lett.* **75**, 1226 (1995).
- [8] H. M. López, J. Gachelin, C. Douarche, H. Auradou, and E. Clément, *Phys. Rev. Lett.* **115**, 028301 (2015).
- [9] J. Urzay, A. Doostmohammadi, and J. M. Yeomans, *Journal of Fluid Mechanics* **822**, 762 (2017).
- [10] S. Rafai, L. Jibuti, and P. Peyla, *Phys. Rev. Lett.* **104**, 098102 (2010).
- [11] J. Prost, F. Jülicher, and J.-F. Joanny, *Nature Physics* **11**, 111 (2015).
- [12] M. Moradi and A. Najafi, *EPL* **109**, 24001 (2015).
- [13] S. Ramaswamy, *Journal of Statistical Mechanics: Theory and Experiment* 2017, **054002** (2017).
- [14] S. Ramaswamy and M. Rao, *New Journal of Physics* **9**, 423 (2007).
- [15] R. Voituriez, J. F. Joanny, J. Prost, *EPL* **70**(3), 404 (2005).
- [16] M. Leoni and T. B. Liverpool, *Phys. Rev. Lett.* **105**, 238102 (2010).
- [17] J. Adler, *Science* **153**, 708 (1966).
- [18] S. Saha, R. Golestanian, and S. Ramaswamy, *Physical Review E* **89**, 062316 (2014).
- [19] I. Theurkauff, C. Cottin-Bizonne, J. Palacci, C. Ybert, and L. Bocquet, *Phys. Rev. Lett.* **108**, 268303 (2012).
- [20] E. F. Keller and L. A. Segel, *Journal of Theoretical Biology* **26**, 399 (1970).
- [21] E. F. Keller and L. A. Segel, *Journal of theoretical biology* **30**, 225 (1971).
- [22] C. Jin, C. Krüger, and C. C. Maass, *Proceedings of the National Academy of Sciences* **114**, 5089 (2017).
- [23] B. Liebchen, D. Marenduzzo, and M. E. Cates, *Phys. Rev. Lett.* **118**, 268001 (2017).
- [24] E. Lushi, R. E. Goldstein, and M. J. Shelley, *Phys. Rev. E* **86**, 040902 (2012).
- [25] J. L. Anderson, *Ann. Rev. Fluid Mech.* **21**, 61 (1989).
- [26] O. Pohl and H. Stark, *Phys. Rev. Lett.* **112**, 238303 (2014).
- [27] G. B. Jeffery, *Proceedings of the royal society of London A: Mathematical, physical and engineering sciences*, **102**, 161 (1922).
- [28] M. Farzin, K. Ronasi, and A. Najafi, *Phys. Rev. E* **85**, 061914 (2012).
- [29] C. M. Pooley, G. P. Alexander, and J. M. Yeomans, *Phys. Rev. Lett.* **99**, 228103 (2007).
- [30] H. Behmadi, Z. Fazli, and A. Najafi, *Journal of Physics: Condensed Matter* **29**, 115102 (2017).
- [31] Z. Fazli, A. Najafi, *J. of Stat. Mech.: Theory and Experiment*, **2**, 023201 (2018).
- [32] K. A. Johnson and R. S. Goody, *Biochemistry* **50**, 8264 (2011).
- [33] P. A. Spiro, J. S. Parkinson, and H. G. Othmer, *PNAS* **94**(14), 7263 (1997).
- [34] C. V. Rao, J. R. Kirby, and A. P. Arkin, *PLoS biology* **2**(2), 49 (2004).
- [35] D. Saintillan and M. J. Shelley, *Phys. Rev. Lett.* **100**, 178103 (2008).
- [36] A. Baskaran and M. C. Marchetti, *Phys. Rev. E* **77**, 011920 (2008).
- [37] A. Baskaran and M. C. Marchetti, *Proceedings of the National Academy of Sciences* **106**, 15567 (2009).
- [38] A. Doostmohammadi, M. F. Adamer, S. P. Thampi, J. M. Yeomans, *Nature communications* **7**, 10557 (2016).
- [39] I. S. Aranson, A. Sokolov, J. O. Kessler, and R. E. Goldstein, *Phys. Rev. E* **75**, 040901 (2007).
- [40] G. Luca, and M. C. Marchetti, *Soft Matter* **8**, 129 (2012).